









Original Article



Antibiotic-Dependent Relationships Between the Nasal Microbiome and Secreted Proteome in Nasal Polyps

Yi-Sook Kim ^{1,2,3} Dohyun Han ⁴ Ji-Hun Mo ^{5,6} Yong-Min Kim ^{6,7}
Dae Woo Kim ^{6,8} Hyo-Guen Choi ⁹ Jong-Wan Park ^{1,2,3,10}
Hyun-Woo Shin ^{1,2,3,6,10,11*}

¹Obstructive Upper airway Research (OUaR) Laboratory, Department of Pharmacology, Seoul National University College of Medicine, Seoul, Korea

²Department of Biomedical Sciences, Seoul National University Graduate School, Seoul, Korea

³Cancer Research Institute, Seoul National University College of Medicine, Seoul, Korea

⁴Proteomics Core Facility, Biomedical Research Institute, Seoul National University Hospital, Seoul, Korea

⁵Department of Otorhinolaryngology-Head and Neck Surgery, Dankook University Hospital, Cheonan, Korea

⁶Clinical Mucosal Immunology Study Group, Seoul, Korea

⁷Department of Otorhinolaryngology-Head and Neck Surgery, Chungnam National University Hospital, Daejeon, Korea

⁸Department of Otorhinolaryngology-Head and Neck Surgery, Boramae Medical Center; Seoul, Korea

⁹Department of Otorhinolaryngology-Head & Neck Surgery, Hallym University College of Medicine, Anyang, Korea

¹⁰Ischemic/Hypoxic Disease Institute, Seoul National University College of Medicine, Seoul, Korea

¹¹Department of Otorhinolaryngology-Head and Neck Surgery, Seoul National University Hospital, Seoul, Korea

OPEN ACCESS

Received: Nov 18, 2020

Revised: Dec 27, 2020

Accepted: Dec 27, 2020

Correspondence to

Hyun-Woo Shin, MD, PhD

Department of Otorhinolaryngology-Head and Neck Surgery, Seoul National University Hospital, 103 Daehak-ro, Jongno-gu, Seoul 03080, Korea.

Tel: +82-2-740-8285

Fax: +82-2-745-7996

E-mail: charlie@snu.ac.kr


Copyright © 2021 The Korean Academy of Asthma, Allergy and Clinical Immunology · The Korean Academy of Pediatric Allergy and Respiratory Disease

This is an Open Access article distributed under the terms of the Creative Commons Attribution Non-Commercial License (<https://creativecommons.org/licenses/by-nc/4.0/>) which permits unrestricted non-commercial use, distribution, and reproduction in any medium, provided the original work is properly cited.


ORCID iDs

Yi-Sook Kim 


<https://orcid.org/0000-0002-6208-6212>

Dohyun Han 


<https://orcid.org/0000-0002-0841-1598>

Ji-Hun Mo 

<https://orcid.org/0000-0003-1331-364X>

Yong-Min Kim 

<https://orcid.org/0000-0001-5414-8332>

Dae Woo Kim 

<https://orcid.org/0000-0001-5166-3072>

ABSTRACT

Purpose: Chronic rhinosinusitis (CRS) is a heterogeneous chronic inflammatory condition of the paranasal sinuses and nasal passages. Although antibiotics are used to reduce inflammation or to treat an episode of acute rhinosinusitis, their effects on the nasal environment and host response in CRS is unclear.

Methods: We analyzed the effects of antibiotics on the nasal microbiome and secreted proteome in CRS using multi-omic analysis. Nasal secretions were collected from 29 controls, 30 CRS patients without nasal polyps (NP), and 40 CRS patients with NP. A total of 99 subjects were divided into 2 groups that included subjects who had taken antibiotics 3 months prior to sampling and those who had not. We performed 16S ribosomal DNA sequence analyses and Orbitrap mass spectrometry-based proteomic analyses. Spearman correlation was used to assess the correlations between the nasal microbiome and secreted proteome.

Results: The associations between the nasal microbiome and secreted proteome were noted in subjects who had used antibiotics. Antibiotics could have stronger effects on their associations in patients with CRS with NP than in those without. It remains unknown whether these holistic changes caused by antibiotics are beneficial or harmful to CRS, however, the associations could be differentially affected by disease severity.

Conclusion: These findings provide new insight into the nasal environment and the host response in CRS.

Keywords: Rhinitis; nasal polyps; metagenomics; proteomics; anti-bacterial agents; sinusitis; microbiota; proteome

Hyo-Guen Choi <https://orcid.org/0000-0003-1655-9549>Jong-Wan Park <https://orcid.org/0000-0003-4676-5191>Hyun-Woo Shin <https://orcid.org/0000-0002-4038-9992>**Disclosure**

There are no financial or other issues that might lead to conflict of interest.

Availability of data and materials

The raw sequence data for the metagenomics are available in the NCBI Sequence Read Archive at study accession number PRJNA557492. The raw data for proteomics have been deposited to Proteome Xchange Consortium via PRIDE partner repository with the accession number PXD018960.

INTRODUCTION

Chronic rhinosinusitis (CRS) is a persistent inflammatory condition of the nasal mucosa and sinus. It is one of the most common upper airway diseases in Western countries and in Asia.¹ This disease exhibits considerable heterogeneity at the clinical and molecular pathophysiologic levels.² Based on this, previous studies have demonstrated that the endotypes of CRS could be characterized based on cytokines,² symptoms,³ microbiota composition,⁴ and clinical characteristics.⁵

Recently, multi-omic analyses were performed to reveal interrelationships among the microbiome, metabolome, transcriptome, and proteome in association with human diseases.⁶ For example, molecular profiles of host (transcriptomics and genomics) and microbial profiles (metagenomics, metaproteomics, and metatranscriptomics) revealed that profiling of disease-associated microbiomes should be accounted for corresponding molecular changes in the host epithelium.⁷ Metagenomic, transcriptomic, and proteomic analyses identified the interactions between the sputum microbiome and host interferon signaling in chronic obstructive pulmonary disease patients.⁸ Therefore, integrative analyses of metagenomics and secreted proteomics in CRS could provide a better understanding of heterogeneity based on associated changes in nasal environment (microbiome) and host response (secreted proteome).

Oral antibiotics were frequently prescribed despite lack of evidence from randomized controlled trials regarding benefit of antibiotics.^{9,10} However, most of previous omics analyses examining CRS did not take the use of antibiotics into account.^{4,11-27} Thus, the effects of antibiotics on nasal microbial communities and host response are largely unknown. Here, we performed metagenomics and proteomics analyses using nasal secretions in healthy control and CRS patients. The subjects were divided into 2 groups that included the subjects who had taken antibiotics 3 months prior to sampling (the ABX group) and those who had not (the NABX group). Furthermore, we sought to gain insight into any potential interactions between the nasal microbiome and the secreted proteome.

MATERIALS AND METHODS

Study design and collection of nasal secretions

The Internal Review Board of Seoul National University Hospital (No. C-1308-099-515) approved this study. All subjects were informed of the purpose of the study, and they all signed written informed consent forms. A diagnosis of CRS was based on patient history, physical examination, nasal endoscopy, and sinus computed tomography in accordance with the 2012 European position paper on rhinosinusitis and nasal polyps guidelines.²⁸ Patients possessing deviated nasal septa but lacking any sinonasal disease were considered as the control. Subjects that were less than 14 years of age and who were diagnosed with unilateral rhinosinusitis, antrochoanal polyps, allergic fungal sinusitis, cystic fibrosis, or immotile ciliary disease were excluded from the study. The demographic characteristics of the subjects are summarized in **Table 1**. Nasal secretions were obtained from both sides of the nose as previously described.²⁹ Sterilized strips of filter paper (7 × 30 mm; Whatman No. 42, Whatman, Clifton, NJ, USA) were placed on the middle meatus for 10 minutes. Two filter papers from each subject were transferred into a tube. Then, 1 mL of nuclease-free water was added to each tube, and the tubes were rotated for 1 hour at room temperature. The nasal secretions were stored in aliquots at -70°C. The workflow is shown in **Supplementary Fig. S1A**.

Table 1. Demographic characteristics of subjects

Characteristic	Control (n = 29)	CRSsNP (n = 30)	CRSwNP (n = 40)	P value*
Male	24 (82.8)	16 (53.3)	27 (67.5)	0.054
Age (yr)	32.4 ± 14.8	41.6 ± 15.1 [‡]	48.8 ± 14.4 [§]	< 0.001
BMI (kg/m ²)	23.3 ± 3.0	23.2 ± 3.4	25.1 ± 4.7	0.171
Smoking	7 (24.1)	4 (13.3)	15 (37.5)	0.072
Atopy	11 (37.9)	7 (24.1)	13 (33.3)	0.515
Polyps	0 (0)	0 (0)	40 (100.0)	< 0.001
Lund-Mackay CT score	0	14.2 ± 6.4 [§]	17.3 ± 4.4 [§]	< 0.001
Antibiotics [†]	2 (6.9)	8 (26.7)	16 (40.0)	0.009
Dental problem	1 (3.4)	2 (6.7)	3 (7.5)	0.774
Asthma	0 (0)	2 (6.7)	2 (5.0)	0.397
Allergic rhinitis	13 (44.8)	12 (40.0)	8 (20.0)	0.063
Methodology				
Metagenomic analysis	29	30	40	
Proteomic analysis	23	24	22	

Data are shown as mean ± standard deviation or number (%).

BMI, body mass index; CT, computed tomography.

*P values based on χ^2 or Kruskal-Wallis test (categorical or continuous variables, respectively); [†]Use of antibiotics in 3 months preceding sampling; [‡]P < 0.05, [§]P < 0.001.

DNA extraction and sequencing

After preparation of nasal secretions, 16S ribosomal DNA (rDNA) was extracted using the PowerSoil DNA Isolation Kit (Mo Bio Laboratories, Inc., Carlsbad, CA, USA). The manufacturer's instructions for the kit were followed for all subsequent procedures. The isolated DNA was sent to Macrogen Corporation (Macrogen Inc., Seoul, Korea) for amplification and sequenced on a Miseq instrument (Illumina, San Diego, CA, USA). A sequencing library was prepared by amplifying the V3-4 region of 16S rDNA. For the amplification, primers 341F (5'-TCG TCG GCA GCG TCA GAT GTG TAT AAG AGA CAG CCT ACG GGN GGC WGC A-3') and 805R (5'-GTC TCG TGG GCT CGG AGA TGT GTA TAA GAG ACA GGA CTA CHV GGG TAT CTA ATC C-3') were used. The library was quantified using TapeStation DNA ScreenTape D1000 (Agilent, Santa Clara, CA, USA) and Picogreen assay. The 16S rDNA libraries were sequenced using the MiSeq platform for 2 × 300 cycles.

Preparation of nasal secretions for proteomics

A 100 μ L aliquot of each nasal secretion was prepared as previously described.²⁹ The samples were centrifuged at 15,000 rpm for 10 minutes at 4°C. We measured the protein concentration in the supernatant by tryptophan fluorescence emission at 350 nm using an excitation wavelength of 295 nm.³⁰ For the analysis, 50 μ g of nasal secreted proteins were used per sample. Proteins were digested using the 2-step FASP procedure with some modifications.^{31,32} Pellets were resuspended in SDT buffer (2% SDS, 10mM TCEP, and 50mM CAA in 0.1M Tris pH 8.0). Then, the solution loaded onto a 10K Amicon filter (Millipore, Burlington, MA, USA). The buffer was exchanged to UA solution (8M urea in 0.1M Tris pH 8.5) using centrifugation at 14,000 g. Following the exchange of 40 mM ammonium bicarbonate (ABC) buffer, proteins were digested at 37°C overnight using a trypsin/LysC mixture (protein-to-protease ratio of 100:1). The peptides were isolated using centrifugation. After the filter units were rinsed with 40 mM ABC, we performed second digestion at 37°C for 2 hours using trypsin (enzyme-to-substrate ratio [w/w] of 1:1,000). The digested peptides were acidified using 10% trifluoroacetic acid and desalted using homemade C18-StageTips as previously described.^{31,32} Finally, we used a vacuum dryer to dry it and stored at -80°C.

High-pH StageTip-based peptide fractionation

For peptide spectrum library, we performed StageTip-based, high-pH peptide fractionation as described with some modifications.³¹ Peptides obtained from pooled samples were dissolved in 200 μ L of loading solution (10 mM ammonium hydroxide solution, pH 10 and 2% acetonitrile) and separated on the reversed-phase tip columns, prepared by packing POROS 20 R2 (Invitrogen, Carlsbad, CA, USA) into a 200 μ L yellow tip with C18 Empore disk membranes (3M, Bracknell, UK) at the bottom. After conditioning of microcolumns with methanol, acetonitrile, and loading buffer, peptides were loaded at pH 10, and 20 fractions were subsequently eluted with buffer solutions, pH 10, containing 5%, 10%, 15%, 20%, 25%, 30%, 35%, 40%, 60%, and 80% acetonitrile. To improve the orthogonal fractionation of the RP-RP separation, 20 fractions were combined into 6 fractions in a noncontiguous manner. The 6 fractions were dried in a vacuum centrifuge and stored at -80°C until liquid chromatography (LC)-mass spectrometry (MS)/MS analysis.

LC-MS/MS analysis

LC-MS/MS analysis was performed using a Q-exactive plus (Thermo Fisher Scientific, Waltham, MA, USA) coupled to an Ultimate 3000 RSLC system (Dionex, Sunnyvale, CA, USA) via a nano electrospray source as described with some modifications.^{29,33} Peptides in samples were separated using the 2-column setup (a trap column [300 μm I.D. \times 5 mm, C18 3 μm , 100 \AA] and an analytical column [50 μm I.D. \times 50 cm, C18 1.9 μm , 100 \AA]). Prior to injection of each sample, we resuspended the dried peptides in solvent A (2% acetonitrile and 0.1% formic acid). After the samples were loaded onto the nano LC, the samples were run with a 90 minutes gradient from 8% to 30% solvent B (80% acetonitrile and 0.1% formic acid). The spray voltage was set to 2.0 kV in the positive ion mode, and the temperature of the heated capillary was 320°C . The MS method consisted of a survey scan at 35,000 resolution from 400 to 1,220 m/z. Automatic gain control (AGC) target of 3×10^6 at injection time of 60 ms. Then, 19 DIA windows were acquired at 35,000 resolution with AGC target 3×10^6 and auto for injection time.³⁴ Stepped collision energy was 10% at 27%.

Data processing for spectral library construction

First, we processed MS raw files that obtained from 18 data-dependent acquisition (DDA) measurements of the pooled samples using MaxQuant (version 1.6.1.0). MS/MS spectra were searched against the Human Uniprot database (December 2014, 88,657 entries) and the Biognosys iRT peptides fasta database using the Andromeda. Data was searched with 6 ppm precursor ion tolerance for total protein level analysis and 20 ppm MS/MS ion tolerance. We used variable modifications (N-acetylation of protein and oxidation of methionine) and a fixed modification (cysteine carbamido-methylation). Enzyme specificity was set as full tryptic digestion. Peptides with a minimum length of 6 amino-acids and up to 2 missed-cleavages were considered. The required false discovery rate (FDR) was set to 1% at the peptide, protein, and modification level. To maximize the number of quantification events across samples, we enabled the 'Match between Runs' option on the MaxQuant platform. MaxQuant search results were imported as spectral libraries into Spectronaut Pulsar X with default settings.

In addition to the typical DDA-based spectral library, we generated a spectral library from the DIA data using the Spectronaut software (Biognosys, Schlieren, Switzerland). The Pulsar search engine integrated in Spectronaut Pulsar X was used to identify peptides and proteins using only independent DIA dataset with the same search engine parameters (fasta database, modifications, peptide length, miss-cleavage, peptide, and protein FDR) as listed above for MaxQuant.

Data processing for the DIA MS

The DIA data of individual samples were analyzed with Spectronaut Pulsar X (Biognosys). First, we converted the DIA raw files into an htrm format by using the GTRMS Converter provided by the Spectronaut. The FDR was estimated with the mProphet³⁵ approach and set to 1% at peptide precursor level and at 1% at protein level. The proteins were inferred by the software, and the quantification information was acquired at the protein level by using the q -value < 0.01 criteria, which was used for subsequent analyses.

Bioinformatic analysis

Raw sequences were analyzed and quality-filtered using Quantitative Insights Into Microbial Ecology (QIIME) (version 1.9.1). An operational taxonomic unit (OTU) was defined at 97% sequence identity using UCLUST against the SILVA reference sequence database (version 132). Singletons were removed from the OTU table to reduce the noise and finally, 12,634,938 sequences remained. Alpha diversity (Chao1, the number of observed OTUs, Shannon, and Simpson) was calculated in QIIME. Beta diversity was calculated using a Bray–Curtis distance matrix with the vegan package in R software. In addition, principal coordinates analysis was performed using the Phyloseq package in R software. Linear discriminant analysis (LDA) effect size (LEfSe) was performed to determine bacterial features most likely to describe differences between groups among all of the identified bacterial families.³⁶ The relative abundance of each OTU was calculated by dividing the read counts of an OTU by the total read counts of all OTUs in each subject, except for read counts of *Archaea*, *Chloroplast* and *Mitochondria*. Proteomic data were normalized using width adjustment. Ingenuity Pathway Analysis (IPA; QIAGEN, Hilden, Germany) software was used to predict canonical pathways. Missing values in proteomic analysis were imputed by normal distribution (width = 0.15, downshift = 1.8) using Perseus. Graphical outputs were visualized using R software (version 3.5.1), Perseus (version 1.6.0), and GraphPad Prism (version 8.1.1).

Statistical analysis

Student's t -test or analysis of variance (ANOVA) was used to compare the data under normal distribution, while Mann-Whitney U or Kruskal-Wallis tests were used for non-parametric analysis. A χ^2 test was used to examine the associations between categorical variables. The significant differences between groups were calculated using permutational multivariate ANOVA (PERMANOVA) via Adonis function in vegan package in R software. LEfSe analysis used the Wilcoxon rank-sum test or Kruskal-Wallis rank-sum test. In IPA analysis, P value of Fisher's exact test < 0.001 was considered significant pathways. Spearman correlation was used to assess the correlation and adaptive sum of powered correlation (aSPC)³⁷ test was used to calculate global association between microbiome and proteome. The statistical analyses were conducted using SPSS ver. 25.0 (SPSS Inc., Chicago, IL, USA), Perseus (version 1.6.0), and R software (version 3.5.1).

RESULTS

Differences in the microbial composition and proteome according to disease status

From our data, we identified 1,329 OTUs at the genus level in 29 controls, 30 CRS without NP (CRSsNP), and 40 CRS with NP (CRSwNP) patients. To determine if the microbial composition was different according to disease status, we analyzed the alpha and beta diversity in a total of 99 subjects. Shannon and Simpson indices were significantly increased

across control to CRSwNP group, while Chao1 and the number of observed OTUs were not increased (Fig. 1A and Supplementary Fig. S2A). There were significant differences in microbial composition in relation to disease status (Fig. 1B). To investigate which bacterial taxa were different in relation to disease status, we compared the nasal bacterial composition. *Firmicutes* and *Bacteroidetes* were significantly increased from the control to

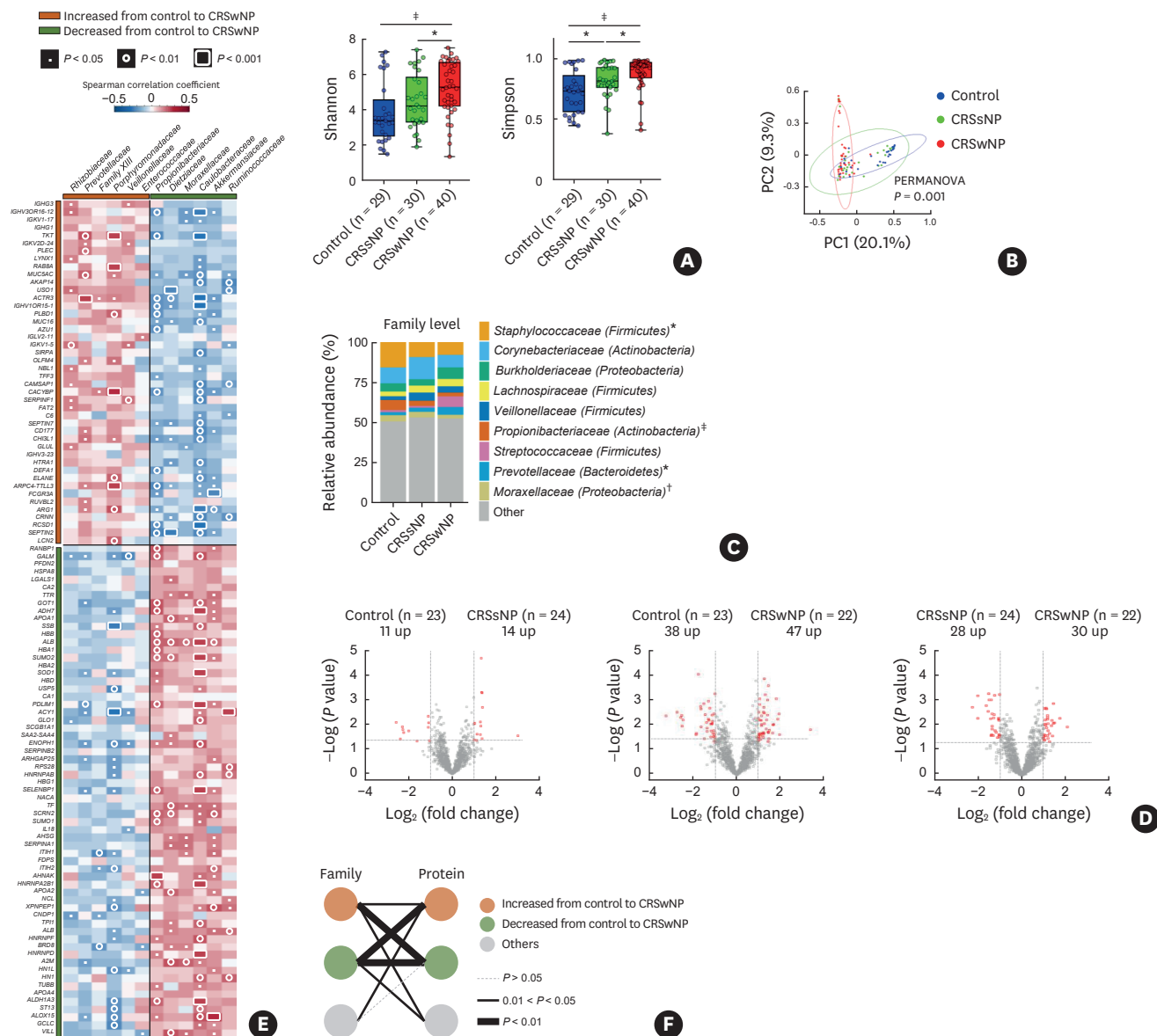


Fig. 1. Nasal microbiome and secreted proteome profiles. (A) Alpha diversity according to disease status (horizontal line = median and whiskers = min/max range). (B) A principal coordinates analysis plot based on Bray-Curtis distance matrix. (C) Distribution of bacterial families. The composition of each family exhibiting a relative abundance of greater than 3 percent is illustrated. The parenthesis represents phylum within the family. (D) Volcano plots of the proteome. The horizontal dashed line indicates P values of 0.05 (Student's t -test), and the vertical dashed lines indicate fold changes of 2.0. (E) Spearman correlation heatmap of secreted proteomes (analysis of variance, $P < 0.05$) and the nasal microbiome (Kruskal-Wallis, $P < 0.05$). The proteome and microbiome were arranged from top to bottom and from left to right in order of the lowest to the highest P value, respectively. Orange and green boxes indicated increased and decreased families and proteins from the control group to the CRSwNP group. Redundant microbiomes and proteomes were excluded from the heatmap. (F) Association between families and proteins. Orange and green circles represent the same groups previously described in (E). Gray circles represent other microbiomes and proteomes that were identified in this study. CRSsNP, chronic rhinosinusitis without nasal polyp; CRSwNP, chronic rhinosinusitis with nasal polyp; PERMANOVA, permutational multivariate analysis of variance. * $P < 0.05$; † $P < 0.01$; ‡ $P < 0.001$.

CRSwNP group, while *Cyanobacteria* levels were significantly decreased from the control to CRSwNP group (**Supplementary Fig. S2B and C**). At the family level, *Staphylococcaceae*, *Propionibacteriaceae*, and *Moraxellaceae* were significantly decreased from the control to CRSwNP group (**Fig. 1C** and **Supplementary Fig. S2D**). *Prevotellaceae* was significantly increased from the control to CRSwNP group. LEfSe analyses revealed *Propionibacteriaceae* and *Moraxellaceae* were the most abundant in the control samples, and *Entomoplasmataceae* was the most abundant in the CRSwNP group at the family level (**Supplementary Fig. S2E**).

To determine if the secreted proteome was different in relation to disease status, we performed proteomic analysis of the nasal secretions of 69 subjects that were divided into 23 control, 24 CRSsNP, and 22 CRSwNP patients. We quantified a total of 2,162 proteins, and on average we quantified approximately 1,440 proteins. The number of quantified proteins from each subject is represented in **Supplementary Fig. S1B**. When comparing the control and CRSsNP groups, relatively small proteomic changes were observed compared to changes observed when comparing the control and CRSwNP groups or CRSsNP and CRSwNP groups (**Fig. 1D** and **Supplementary Table S1**). Given that the nasal microbiome and secreted proteome were different in relation to disease status, we hypothesized that they could correlate with each other. To confirm this hypothesis, we divided the nasal microbiome into 2 groups that included families with increased relative abundance from the control to CRSwNP group (IFc) and families exhibiting decreased relative abundance from the control to CRSwNP group (DFc) (Kruskal-Wallis, $P < 0.05$). We also divided the secreted proteome into 2 groups that included proteins with increased normalized intensity from the control to CRSwNP group (IPc) and proteins exhibiting decreased normalized intensity from the control to CRSwNP group (DPc) (ANOVA, $P < 0.05$). A number of significant positive or negative correlations were observed among the groups (IFc, DFc, IPc, and DPc) (**Fig. 1E**). To confirm the associations among the 4 groups, we applied aSPC tests. These analyses revealed significant global association among the groups (IFc, DFc, IPc, and DPc) (aSPC test, $P < 0.01$) (**Fig. 1F**). In contrast, less significant correlations were detected between each group (IFc, DFc, IPc, and DPc) and others in regard to the microbiome and proteome, respectively (aSPC test, $P > 0.01$). These findings suggest a strong association between the nasal microbiome and the secreted proteome according to disease status.

Differential microbiome composition according to the use of antibiotics

Further, we sought to examine variations in the microbial community in relation to disease status in the NABX and ABX groups. The NABX group consisted of 27 controls, 22 CRSsNP, and 24 CRSwNP patients, while the ABX group consisted of 2 controls, 8 CRSsNP, and 16 CRSwNP patients. In the NABX group, unlike Chao1 and the number of observed OTUs, the Shannon and Simpson indices were significantly increased from the control to the CRSwNP group (**Fig. 2A** and **Supplementary Fig. S3A**). A clearly identifiable clustering was observed in the NABX group (**Supplementary Fig. S3C**); however, in the ABX group, there were no significant differences in the alpha and beta diversities (**Fig. 2B** and **Supplementary Fig. S3B and D**).

Next, we compared the nasal bacterial composition in the NABX and ABX groups. In the NABX group, *Firmicute*, *Cyanobacteria*, and *Bacteroidetes* significantly differed according to disease status (**Supplementary Fig. S4A and C**). At the family level, the relative abundance of *Propionibacteriaceae*, *Moraxellaceae*, and *Prevotellaceae* significantly differed according to disease status in the NABX group (**Fig. 2C** and **Supplementary Fig. S4D**). LEfSe analysis revealed that *Propionibacteriaceae* was significantly decreased in the CRSwNP and CRSsNP groups compared to levels in the control group (**Supplementary Fig. S4E**). In the ABX group, there was no significant

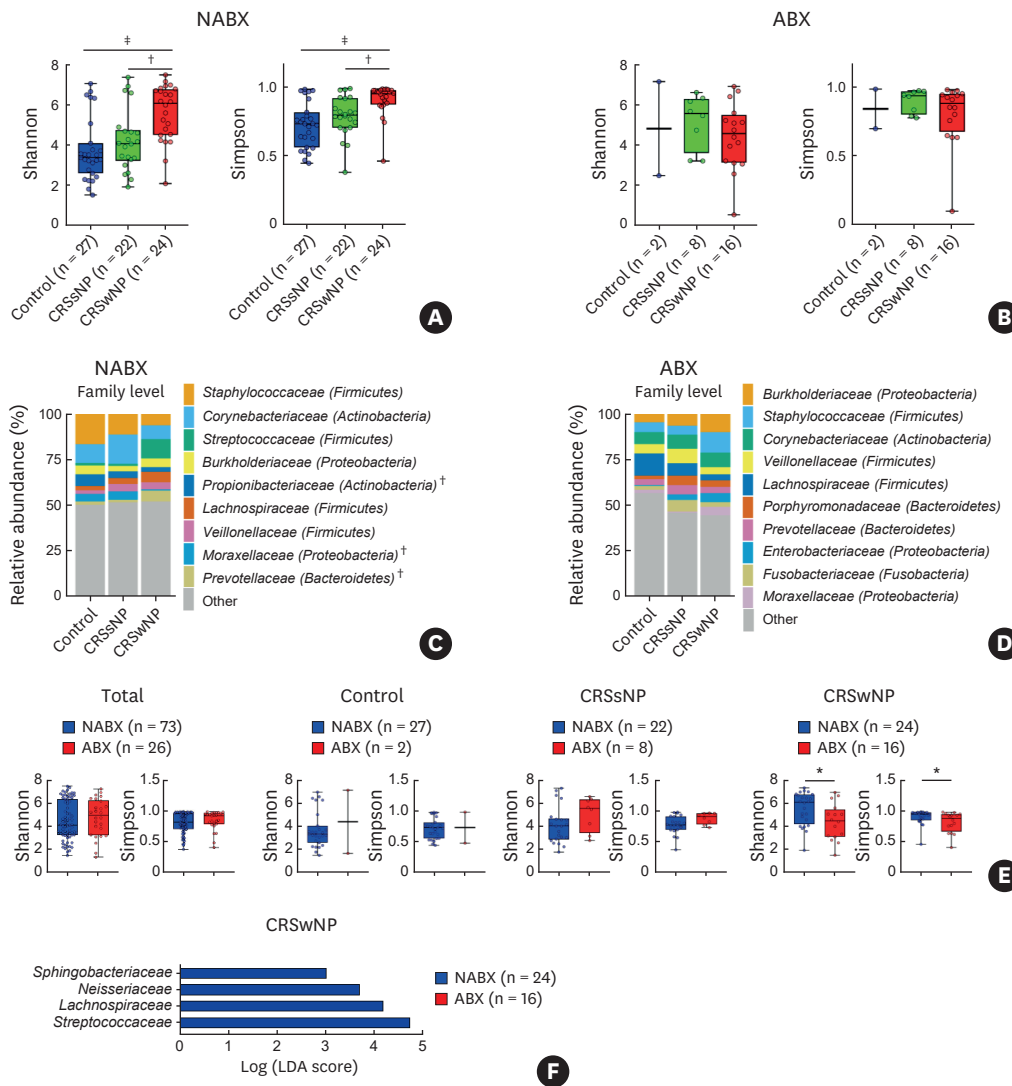


Fig. 2. Differential microbial composition according to the use of antibiotics. (A, B) Comparison of Shannon and Simpson indices according to disease status in the NABX and ABX groups. (C, D) Distribution of bacterial families according to disease status in the NABX and ABX groups. The composition of each family exhibiting a relative abundance of greater than 3 percent is illustrated. The parenthesis indicates phylum within the family. (E) Comparison of Shannon and Simpson indices between the NABX and ABX groups using a total of 99 subjects, controls, CRSSNP, and CRSwNP patients, respectively (horizontal line = median and whiskers = min/max range). (F) LDA effect size analysis identified the NABX group-enriched families and the ABX group-enriched families in CRSwNP patients. The plot indicates taxa with an LDA score > 3.0 and a $P < 0.05$ in all-against-all comparisons (more stringent). ABX, the subjects who had taken antibiotics 3 months before sampling; NABX, the subjects who had not taken antibiotics 3 months before sampling; CRSSNP, chronic rhinosinusitis without nasal polyp; CRSwNP, chronic rhinosinusitis with nasal polyp; LDA, linear discriminant analysis. * $P < 0.05$; † $P < 0.01$; ‡ $P < 0.001$.

difference in phyla and families that possessed a relative abundance of greater than 3 percent (Fig. 2D and Supplementary Fig. S4B). When all identified families were analyzed using LfSe, we observed that *Peptostreptococcaceae*, *Desulfovibrionaceae*, and *Alteromonadaceae* were the most dominant families in the control group (Supplementary Fig. S4F). *Sulfurovaceae* was found to be significantly enriched in the CRSSNP group. Taken together, these findings indicate that antibiotic use could reduce differences in microbial communities according to disease status.

To determine the differences in the microbial community resulting from antibiotic use, we compared between the NABX and ABX groups in regard to each disease status. In a total

of 99 subjects, unlike alpha diversities, PERMANOVA revealed that microbial composition significantly differed between the NABX and ABX groups (**Fig. 2E** and **Supplementary Fig. S5A and B**). Among bacterial families with a relative abundance of more than 3%, *Staphylococcaceae*, *Propionibacteriaceae*, and *Streptococcaceae* exhibited significant differences between the 2 groups (**Supplementary Fig. S5C**). In all families that we identified, we found that *Staphylococcaceae*, *Streptococcaceae*, and *Propionibacteriaceae* were significantly decreased in the ABX group compared to levels in the NABX group (**Supplementary Fig. S5D**). *Entothionellaceae* and *Sandaracinaceae* were significantly enriched in the ABX group compared to levels in the NABX group.

Then, we compared the microbial communities between the ABX and NABX groups in the control group. There were no significant differences in alpha and beta diversities between the 2 groups (**Fig. 2E** and **Supplementary Fig. S5E and F**). Additionally, families with a relative abundance of more than 3% were not significantly different between the 2 groups (**Supplementary Fig. S5G**). LEfSe analysis indicated that antibiotic use led to enrichment of families whose relative abundance was lower than 3% (**Supplementary Fig. S5H**). In CRSsNP patients, the alpha diversity indices and microbial composition did not significantly differ between the NABX and ABX groups (**Fig. 2E** and **Supplementary Fig. S6A and B**). Among the families with a relative abundance of more than 3%, *Staphylococcaceae* was significantly decreased in the ABX group compared to levels in the NABX group (**Supplementary Fig. S6C**). LEfSe analysis that was performed on all identified families revealed that *Staphylococcaceae*, *Intrasporangiaceae*, and *Neisseriaceae* were significantly decreased in the ABX group compared to levels in the NABX group (**Supplementary Fig. S6D**). Additionally, *Prevotellaceae* and *Legionellaceae* were enriched significantly in the ABX group compared to levels in the NABX group. Last, we compared the microbial communities between the NABX and ABX groups in CRSwNP patients. Unlike Chao1 and the number of observed OTUs, Shannon and Simpson indices were significantly lower in the ABX group compared to those in the NABX group (**Fig. 2E** and **Supplementary Fig. S6E**). Additionally, PERMANOVA revealed significant differences in microbial composition between the 2 groups (**Supplementary Fig. S6F**). According to these results, it appeared that antibiotics exerted stronger effects on the microbial community in CRSwNP patients compared to those in the control and CRSsNP patients. Among the bacterial families with more than 3% relative abundance, *Streptococcaceae* and *Lachnospiraceae* were significantly decreased in the ABX group compared to levels in the NABX group (**Supplementary Fig. S6G**). In all identified families, LEfSe analysis revealed that *Streptococcaceae*, *Lachnospiraceae*, and *Neisseriaceae* were significantly decreased in the ABX group compared to levels in the NABX group (**Fig. 2F**).

Differences in secreted proteome according to the use of antibiotics

Next, we compared host responses to antibiotics in the non-NP group which consisted of control subjects and CRSsNP patients and the NP group which consisted of CRSwNP patients using proteomic analysis. In the ABX group, relatively small proteomic changes were observed between the non-NP and NP groups compared to those in the NABX group (**Fig. 3A**). This was consistent with our results indicating that the use of antibiotics reduced differences in microbial communities according to disease status. As shown in **Supplementary Tables S2**, proteins with a fold change ≥ 2.0 at a P value < 0.05 in the NABX group were considerably different compared to those in the ABX group.

Furthermore, to determine the differences in the secreted proteome based on antibiotic use, we compared between the NABX and ABX groups in total of subjects, the non-NP and the

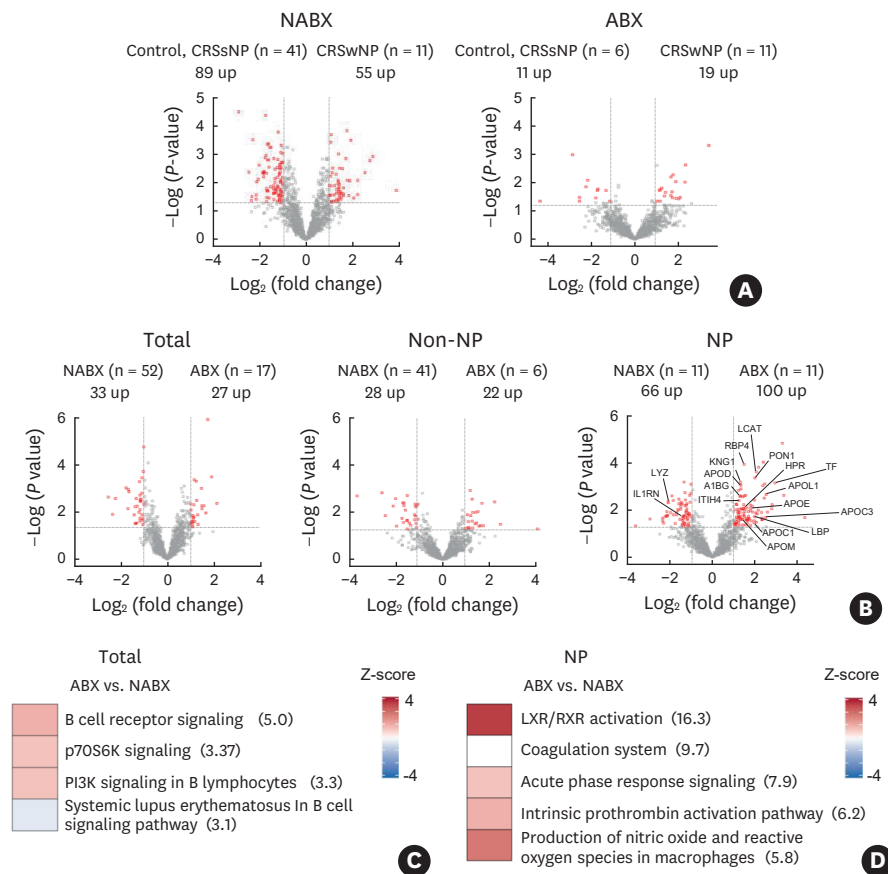


Fig. 3. Differences in the secreted proteome according to the use of antibiotics. (A, B) Volcano plots of the secreted proteome where \log_2 of fold changes was plotted versus the $-\log_{10}$ of the P values from the Student's t -test. The horizontal dashed line indicates P values of 0.05, and the vertical dashed lines indicate fold changes of 2.0. Red squares represent proteins with a fold change ≥ 2.0 at P value < 0.05 . In the NP group, the labeled squares indicate proteins involved in LXR/RXR activation. (C, D) Canonical pathway analysis representing significantly up- or down-regulated pathways in the ABX group compared to those in the NABX group. The pathways with P values smaller than 0.001 were arranged from top to bottom in order of the lowest to the highest P value. The parenthesis represented the $-\log_{10} P$ value. ABX, the subjects who had taken antibiotics 3 months before sampling; NABX, the subjects who had not taken antibiotics 3 months before sampling; CRSsNP, chronic rhinosinusitis without nasal polyp; CRSwNP, chronic rhinosinusitis with nasal polyp; NP, nasal polyps.

NP groups (Fig. 3B and Supplementary Table S3). Based on previous results obtained using metagenomics, it was shown that antibiotics could exert stronger effects on the secreted proteome in the NP group compared to that in total and the non-NP group. We tried to identify the canonical pathways, which were most significantly involved with the proteins that exhibited a fold change ≥ 2.0 at a P value < 0.05 in each group, using IPA. When examining all subjects, the pathways were completely different from those identified in the NP group, as the pathways were associated with innate immunity and production nitric oxide (NO) and reactive oxygen species (ROS) (Fig. 3C and D). There was no significant pathway found in the non-NP group ($P > 0.001$). As LXR/RXR activation was the most significant pathway according to IPA analysis, proteins associated this pathway were labeled in a volcano plot derived from the NP group (Fig. 3B). These analyses indicated that the use of antibiotics may result in stronger effects on the nasal microbiome and the secreted proteome in the NP group compared to those in the non-NP group.

Antibiotic-dependent relationships between nasal microbiome and secreted proteome

We next sought to investigate if the associations between the microbiome and the secreted proteome may differ according to antibiotic use. If associations with a high number of significant correlations were altered by exposure to antibiotics, this would be meaningful. Therefore, we arranged the microbiome and secreted proteome in descending order from the highest to the lowest number of significant correlations with each other (Supplementary Fig. S7A and B). Among these, we clustered the top 25 percent of the microbiome and secreted proteome in the NABX and ABX groups (Fig. 4A and B). The average R -squared value in the

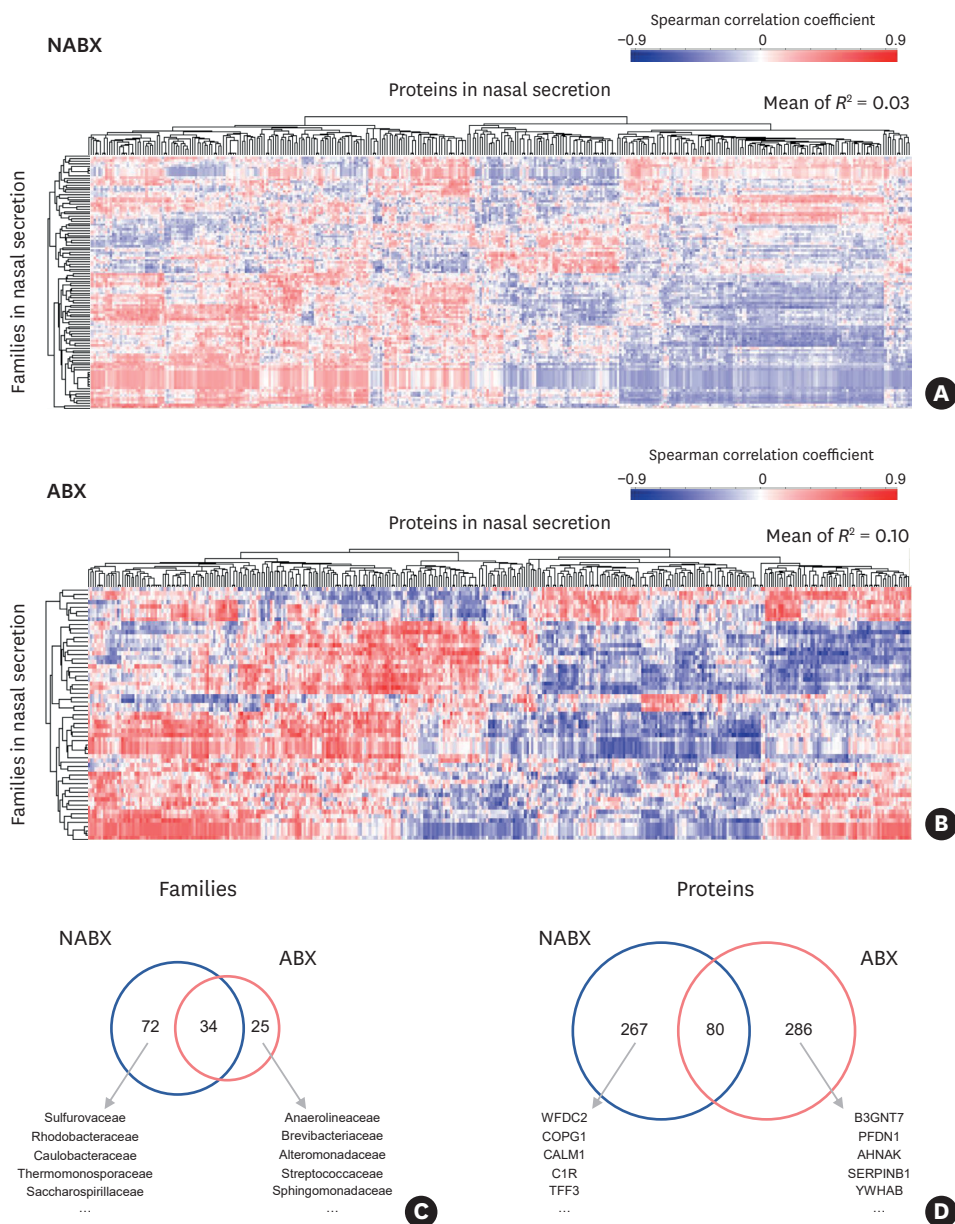


Fig. 4. Antibiotic-dependent relationships between the nasal microbiome and the secreted proteome. (A, B) Hierarchical clustering of the top 25 percent of the microbiome and proteome with a high number of significant correlations in the NABX and ABX groups. The means of squared coefficients were calculated using all values presented in (A, B). Among the microbiomes and proteomes identified in (A, B), a Venn diagram reveals the number of families (C) and proteins (D) in the NABX and ABX groups. The top 5 proteins and families (non-overlapping and non-redundant) are represented. ABX, the subjects who had taken antibiotics 3 months before sampling; NABX, the subjects who had not taken antibiotics 3 months before sampling.

ABX was higher than that in the NABX group. From these analyses, we confirmed that the microbiome and secreted proteome in the ABX group correlated tightly with one another compared to the correlation observed in the NABX group. Furthermore, among these top 25 percent microbiome and secreted proteome components in the NABX and ABX groups, there was little overlap between the NABX and ABX groups (**Fig. 4C and D**). Likewise, the use of antibiotics altered the associations between the microbiome and secreted proteome. Moreover, their correlations were strengthened in subjects who had taken antibiotics.

Antibiotic-dependent relationships between the nasal microbiome and the secreted proteome in the non-NP and NP groups

Finally, given that antibiotics may exert different effects on the nasal microbiome, secreted proteome, and their association according to disease status, we hypothesized that the associations were altered by antibiotics could differ according to disease status. To confirm this hypothesis, we divided the nasal microbiome into 2 groups that included families with increased relative abundance in the ABX group (IFa) and families with decreased relative abundance in the ABX group (DFa). We also divided the secreted proteome into 2 groups that included proteins with increased normalized intensity in the ABX group (IPa) and proteins with decreased normalized intensity in the ABX group (DPa). We could not detect the IFa group in the NP group. A number of significant positive or negative correlations were observed among the 4 groups (IFa, DFa, IPa and DPa) in both the non-NP and NP groups (**Fig. 5A and B**). We confirmed that the NP group showed stronger correlations with each other than those in the non-NP group. To confirm the associations among the 4 groups, we performed aSPC tests (**Fig. 5C**). The associations between DFa and IPa or DFa and DPa in the NP group were more significant than those observed in the non-NP group; however, we found no correlation between each group (IFa, DFa, IPa and DPa) and others in regard to the microbiome and the proteome. These analyses indicated that the associations between the microbiome and the proteome that were altered by antibiotics were stronger in the NP than in the non-NP group.

DISCUSSION

To our knowledge, this is the first report to analyze the effects of antibiotics on the microbiome, secreted proteome, and their associations in CRS using multi-omics. The relatively large number of subjects used for this study enabled us to more fully understand the associations between CRS and antibiotics. As expected, antibiotic use could reduce differences in the microbial community and the secreted proteome according to disease status. Interestingly, antibiotics may exert strong effects on not only the nasal microbiome and secreted proteome, but also their associations in CRSwNP patients compared to that in CRSsNP patients. Additionally, their correlations were strengthened in subjects who had taken antibiotics.

Previous studies examining the nasal microbiome resulted in inconsistent outcomes for alpha diversity indices in CRS patients compared to those in the control group. Some studies reported that there was no significant difference in alpha diversity between controls and CRS patients.^{13,15,26} Meanwhile, other studies reported that the alpha diversity indices significantly decreased in CRS patients compared to those in the control group.^{4,23,24} Some studies have reported that bacterial diversity was increased in CRS patients compared to controls.^{16,19,25} Moreover, a number of previous studies^{11,12,17,18,21} indicated that alpha diversity was increased,

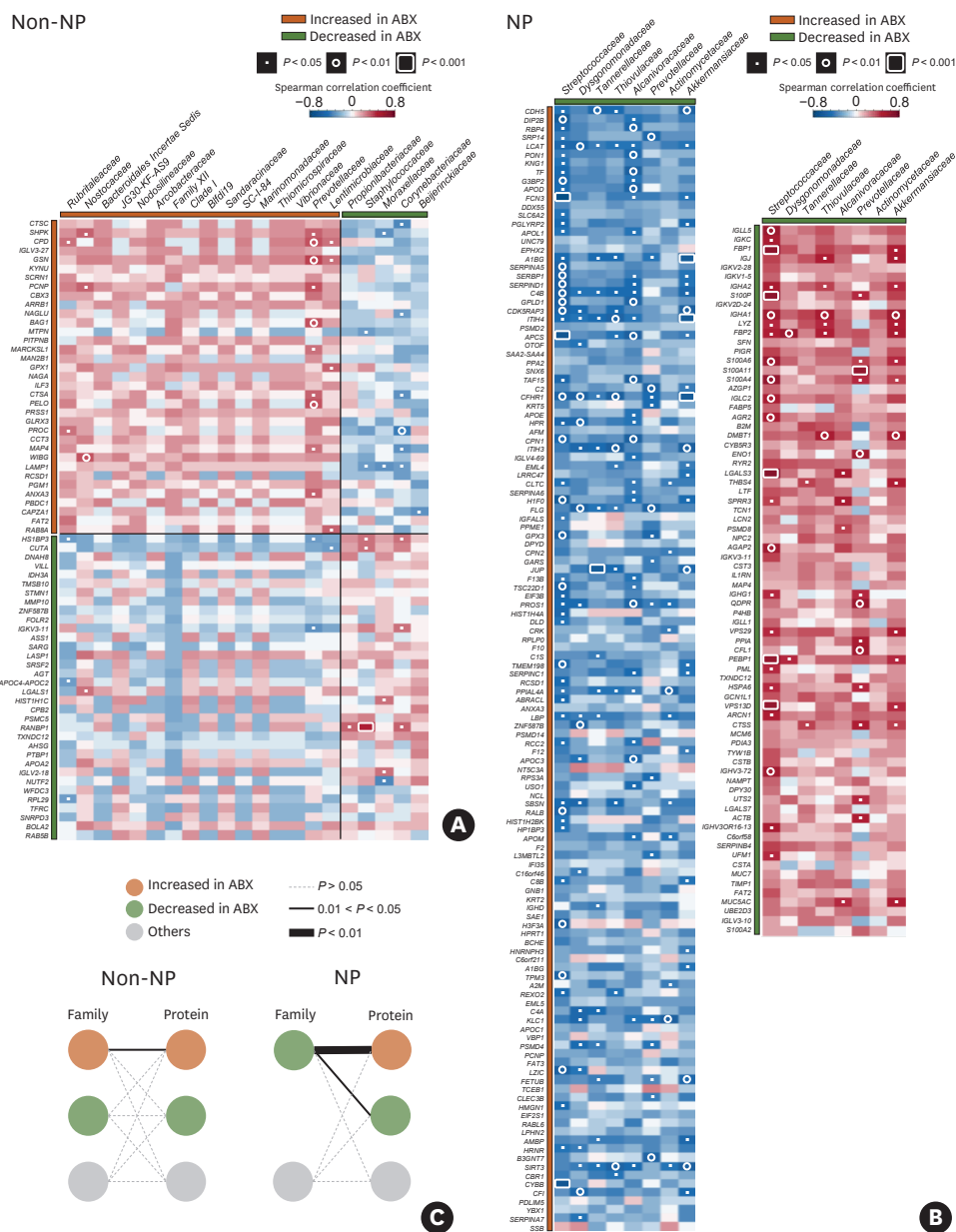


Fig. 5. Antibiotic-dependent relationships between the nasal microbiome and the secreted proteome in controls, CRSsNP, and CRSwNP patients. (A, B) Spearman correlation heatmaps of the secreted proteomes (rows) and the nasal microbiomes (columns) that exhibit significant differences between the NABX and ABX groups in the non-NP and NP groups. The proteome (Student's *t*-test, $P < 0.05$) and microbiome (Mann-Whitney *U* test, $P < 0.05$) were arranged from top to bottom and from left to right in order of the lowest to the highest *P* value. Orange and green boxes indicate families and proteins enriched in the ABX and NABX groups. Redundant microbiomes and proteomes were excluded from the heatmap. (C) Associations between the microbiome and the proteome. Orange and green circles represent the same groups as described in (A, B), respectively. Gray circles indicate other microbiomes and proteomes that were identified in this study (adaptive sum of powered correlation test, $P < 0.05$). ABX, the subjects who had taken antibiotics 3 months before sampling; NABX, the subjects who had not taken antibiotics 3 months before sampling; CRSsNP, chronic rhinosinusitis without nasal polyp; CRSwNP, chronic rhinosinusitis with nasal polyp; NP, nasal polyps.

decreased, or unchanged in CRS patients compared to that in controls, and this was dependent upon the alpha diversity index. These studies generally excluded patients who had taken antibiotics within approximately 1 month prior to sampling, although oral antibiotics

were frequently prescribed for treating symptoms of CRS. A study has demonstrated that microbial richness within the gut was significantly decreased at approximately 6 months following antibiotic treatment.³⁸ Therefore, the differences in alpha diversity according disease status could not be clearly identified in the previous metagenomic studies in CRS patients. In our study that included subjects who had taken antibiotics within 3 months, Shannon and Simpson indices were significantly increased from control to CRSwNP patients (**Fig. 1A**), and we are confident that these results reflect real-world criteria. Based on this, antibiotic use should be taken into account when comparing diversity according to disease status.

We revealed that antibiotics could have differential effects on the associations between the NP and non-NP groups. Antibiotics may exert strong effects on not only the nasal microbiome and secreted proteome, respectively, but also their associations in CRSwNP patients. However, the mechanisms by which antibiotics could differentially affect the microbiome according to disease status. In CRSwNP, tight junction integrity and barrier function were defective,^{39,40} moreover, epithelial repair rate was significantly low compared to control and CRSsNP.⁴¹ Thus, we speculated that the differential effects according to disease status could be caused by defective barrier functions in the NP group. One study has reported a simple quantitative model based on a stability landscape framework.⁴² They demonstrated that the microbiome existed in multiple stable equilibria of landscape that could be influenced by sufficiently strong perturbations such as antibiotics that could alter the microbiome from its normal equilibrium to other states. We guessed that perturbation by antibiotics could shift the microbiome towards equilibrium possessing a different value of alpha diversity (lower diversity) in only the NP group. On the other hands, treatment with antibiotics disrupted the intestinal tight junction.⁴³ Levofloxacin, a commonly used antibiotic for upper airway infections, simulated ROS and caspase-3 activity in cultured human sinonasal epithelial cells.⁴⁴ Therefore, we speculated that the defective barrier functions in CRSwNP patients could make it easier to deliver antibiotics to sinus. Consequently, effects of antibiotics could be differentially affected by disease status.

The IPA analysis revealed that B cell-associated pathways and anti-microbial pathways were more highly activated in the ABX group compared to levels in the NABX group in the total subjects population and the NP group, respectively (**Fig. 3C and D**). PI3K regulated B cell receptor-mediated antigen presentation and airway remodeling.⁴⁵ Activated B cells utilized mTORC1 to activate p70 ribosomal S6 kinase (p70S6K), and this preceded antibody synthesis.⁴⁶ In contrast, macrophages that released proinflammatory cytokines played an important role in clearing bacteria, and this was accompanied by the production of NO and ROS upon contact with pathogens.^{47,48} Several studies have reported that LXR activation exerted anti-inflammatory functions⁴⁹ and inhibited bacterial infection of host macrophages.⁵⁰ Based on these results, antibiotics could contribute to decreased inflammation in nasal cavity. As mentioned above, Shannon and Simpson indices were significantly increased from control to CRSwNP patients (**Fig. 1A**). However, only in the NP group, alpha diversity indices were significantly decreased in subjects who have taken antibiotics compared to subjects who have not (**Fig. 2E**). Therefore, we speculated that antibiotics might exert beneficial effects for CRSwNP patients.

There were some limitations in this present research study. As antibiotics are generally used for treating symptoms of CRS, the number of subjects who taken antibiotics was smaller in the control group than in the CRSsNP and CRSwNP groups. Thus, further studies with a similar proportion of subjects who had taken antibiotics and a larger sample size for each

disease status will be required to verify the association between CRS and antibiotics. The results also need to be further investigated by cohort study.

In summary, integrative analyses reveal that the associations between the nasal microbiome and secreted proteome could be strengthened in subjects who taken antibiotics. Especially, antibiotics could have differential effects on the associations between the NP and the non-NP groups. We demonstrate antibiotics may exert strong effects on not only the nasal microbiome and secreted proteome, respectively, but also their associations in the NP group. It is still unknown whether these holistic changes caused by antibiotics are beneficial or harmful to CRS, however, the associations could be differentially affected by disease status. We suggest that the use of antibiotics need to be considered as a principal confounding factor when the metagenomic or proteomics studies, especially in CRSwNP patients. These findings provide new insight into the nasal environment and the host response in CRS.

ACKNOWLEDGMENTS

This research was supported by grants of the Korea Health Technology R&D Project through the Korea Health Industry Development Institute (KHIDI), funded by the Ministry of Health & Welfare, Republic of Korea (grant number: HI15C2310) and by a grant from the National Research Foundation of Korea (2020R1A4A2002903).

SUPPLEMENTARY MATERIALS

Supplementary Table S1

Identification of differentially expressed proteins with fold change ≥ 2.0 and P value < 0.05 between disease status

[Click here to view](#)

Supplementary Table S2

Identification of differentially expressed proteins with fold change ≥ 2.0 and P value < 0.05 between the non-NP and NP groups in the NABX and ABX groups

[Click here to view](#)

Supplementary Table S3

Identification of differentially expressed proteins with fold change ≥ 2.0 and P value < 0.05 between the NABX and ABX groups in total, the non-NP group and the NP group

[Click here to view](#)

Supplementary Fig. S1

Overview of the study and number of the quantified proteins in each group. (A) Overview of study design. (B) A bar plot of total number of the quantified proteins from the 2 technical replicates in proteomics. Error bars represented the standard deviation of the mean.

[Click here to view](#)

Supplementary Fig. S2

Comparison of diversity and microbial composition among controls, CRSsNP, and CRSwNP patients. (A) Comparison of Chao1 and the number of observed operational taxonomic units between disease status (horizontal line = median and whiskers = min/max range). (B) Distribution of bacterial phyla between disease status. The composition of each phylum with relative abundance of more than 3 percent were illustrated. Among the taxa with relative abundance of more than 3 percent, the dot plots showed relative abundance of phyla (C) and families (D) with significant differences between disease status (horizontal line = mean). (E) LDA effect size analysis identified control group-enriched families (colored in blue), CRSsNP group-enriched families (colored in green), and CRSwNP group-enriched families (colored in red). The plot showed taxa with LDA score > 3.0 and $P < 0.05$ in all-against-all (more stringent).

[Click here to view](#)

Supplementary Fig. S3

Comparison of microbial composition between disease status according to the use of antibiotics. (A, B) Comparison of Chao1 and the number of observed operational taxonomic units between disease status in the NABX and ABX groups (horizontal line = median and whiskers = min/max range). (C, D) Principal coordinates analysis plots based on Bray–Curtis distance matrix in the NABX and ABX groups.

[Click here to view](#)

Supplementary Fig. S4

Phylum and family composition between disease status according to the use of antibiotics. (A, B) Distribution of bacterial phyla between disease status. The composition of each phylum with relative abundance of more than 3 percent were illustrated in the NABX and ABX groups. (C) Among the taxa with relative abundance of more than 3 percent, the dot plot showed relative abundance of phyla with significant differences between disease status in the NABX group (horizontal line = mean). (D) Among the taxa with relative abundance of more than 3 percent, the dot plot showed relative abundance of families with significant differences between disease status in the NABX group (horizontal line = mean). (E, F) LDA effect size analysis identified control group-enriched families (colored in blue), CRSsNP group-enriched families (colored in green), and CRSwNP group-enriched families (colored in red) in the NABX and ABX groups. The plot showed taxa with LDA score > 3.0 and $P < 0.05$ in all-against-all (more stringent).

[Click here to view](#)

Supplementary Fig. S5

Differences in microbial composition according to the use of antibiotics in total of 99 subjects and the control group. Comparison of Chao1 and the number of observed OTUs between the NABX and ABX groups in (A) 99 patients and (E) the control group (horizontal line = median and whiskers = min/max range). (B, F) A Principal coordinates analysis plot based on Bray–Curtis distance matrix. (C, G) Distribution of bacterial families between the NABX and ABX groups. The composition of each family with relative abundance of more than 3 percent were illustrated. The parenthesis indicated phylum belonged to the family. (D and H) LDA effect size analysis identified the NABX group-enriched families (colored in blue) and

the ABX group-enriched families (colored in red). The plot showed taxa with LDA score > 3.0 and $P < 0.05$ in all-against-all (more stringent).

[Click here to view](#)

Supplementary Fig. S6

Differences in microbial composition according to the use of antibiotics in CRSsNP and CRSwNP patients. Comparison of Chao1 and the number of observed OTUs between the NABX and ABX groups in (A) CRSsNP and (E) CRSwNP patients (horizontal line = median and whiskers = min/max range). (B, F) A Principal coordinates analysis plot based on Bray–Curtis distance matrix. (C, G) Distribution of bacterial families between the NABX and ABX group. The composition of each family with relative abundance of more than 3 percent were illustrated. The parenthesis indicated phylum belonged to the family. (D) LDA effect size analysis identified the NABX group-enriched families (colored in blue) and the ABX group-enriched families (colored in red). The plot showed taxa with LDA score > 3.0 and $P < 0.05$ in all-against-all (more stringent).

[Click here to view](#)

Supplementary Fig. S7

Associations between microbiome and proteins in nasal secretions. Spearman correlation heatmaps of total nasal microbiome (columns) and secreted proteome (row) in the NABX (A) and ABX (B) groups. The microbiome and proteome were arranged from top to down and from left to right, respectively, in order of the highest to the lowest number of significant correlations with each other. Black boxes indicated the top 25 percent microbiome and proteome with high number of significant correlations each other.

[Click here to view](#)

REFERENCES

1. Zhang Y, Gevaert E, Lou H, Wang X, Zhang L, Bachert C, et al. Chronic rhinosinusitis in Asia. *J Allergy Clin Immunol* 2017;140:1230-9.
[PUBMED](#) | [CROSSREF](#)
2. Tomassen P, Vandeplass G, Van Zele T, Cardell LO, Arebro J, Olze H, et al. Inflammatory endotypes of chronic rhinosinusitis based on cluster analysis of biomarkers. *J Allergy Clin Immunol* 2016;137:1449-1456.e4.
[PUBMED](#) | [CROSSREF](#)
3. Divekar R, Patel N, Jin J, Hagan J, Rank M, Lal D, et al. Symptom-based clustering in chronic rhinosinusitis relates to history of aspirin sensitivity and postsurgical outcomes. *J Allergy Clin Immunol Pract* 2015;3:934-940.e3.
[PUBMED](#) | [CROSSREF](#)
4. Cope EK, Goldberg AN, Pletcher SD, Lynch SV. Compositionally and functionally distinct sinus microbiota in chronic rhinosinusitis patients have immunological and clinically divergent consequences. *Microbiome* 2017;5:53.
[PUBMED](#) | [CROSSREF](#)
5. Liao B, Liu JX, Li ZY, Zhen Z, Cao PP, Yao Y, et al. Multidimensional endotypes of chronic rhinosinusitis and their association with treatment outcomes. *Allergy* 2018;73:1459-69.
[PUBMED](#) | [CROSSREF](#)
6. Misra BB, Langefeld CD, Olivier M, Cox LA. Integrated omics: tools, advances, and future approaches. *J Mol Endocrinol* 2018;62:R21-45.
[PUBMED](#) | [CROSSREF](#)

7. Lloyd-Price J, Arze C, Ananthakrishnan AN, Schirmer M, Avila-Pacheco J, Poon TW, et al. Multi-omics of the gut microbial ecosystem in inflammatory bowel diseases. *Nature* 2019;569:655-62.
[PUBMED](#) | [CROSSREF](#)
8. Wang Z, Maschera B, Lea S, Kolsum U, Michalovich D, Van Horn S, et al. Airway host-microbiome interactions in chronic obstructive pulmonary disease. *Respir Res* 2019;20:113.
[PUBMED](#) | [CROSSREF](#)
9. Barshak MB, Durand ML. The role of infection and antibiotics in chronic rhinosinusitis. *Laryngoscope Investig Otolaryngol* 2017;2:36-42.
[PUBMED](#) | [CROSSREF](#)
10. Smith SS, Evans CT, Tan BK, Chandra RK, Smith SB, Kern RC. National burden of antibiotic use for adult rhinosinusitis. *J Allergy Clin Immunol* 2013;132:1230-2.
[PUBMED](#) | [CROSSREF](#)
11. Gan W, Yang F, Tang Y, Zhou D, Qing D, Hu J, et al. The difference in nasal bacterial microbiome diversity between chronic rhinosinusitis patients with polyps and a control population. *Int Forum Allergy Rhinol* 2019;9:582-92.
[PUBMED](#) | [CROSSREF](#)
12. Rom D, Bassiouni A, Eykman E, Liu Z, Paramasivan S, Alvarado R, et al. The association between disease severity and microbiome in chronic rhinosinusitis. *Laryngoscope* 2019;129:1265-73.
[PUBMED](#) | [CROSSREF](#)
13. Mahdavinia M, Engen PA, LoSavio PS, Naqib A, Khan RJ, Tobin MC, et al. The nasal microbiome in patients with chronic rhinosinusitis: analyzing the effects of atopy and bacterial functional pathways in 111 patients. *J Allergy Clin Immunol* 2018;142:287-290.e4.
[PUBMED](#) | [CROSSREF](#)
14. Biswas K, Cavubati R, Gunaratna S, Hoggard M, Waldvogel-Thurlow S, Hong J, et al. Comparison of subtyping approaches and the underlying drivers of microbial signatures for chronic rhinosinusitis. *MSphere* 2019;4:e00679-18.
[PUBMED](#) | [CROSSREF](#)
15. Paramasivan S, Bassiouni A, Shiffer A, Dillon MR, Cope E, Cooksley C, et al. The international sinonasal microbiome study (ISMS): a multi centre, international characterization of sinonasal bacterial ecology. *bioRxiv*. Forthcoming 2019.
[CROSSREF](#)
16. Copeland E, Leonard K, Carney R, Kong J, Forer M, Naidoo Y, et al. Chronic rhinosinusitis: potential role of microbial dysbiosis and recommendations for sampling sites. *Front Cell Infect Microbiol* 2018;8:57.
[PUBMED](#) | [CROSSREF](#)
17. Chalermwatanachai T, Vilchez-Vargas R, Holtappels G, Lacoere T, Jáuregui R, Kerckhof FM, et al. Chronic rhinosinusitis with nasal polyps is characterized by dysbacteriosis of the nasal microbiota. *Sci Rep* 2018;8:7926.
[PUBMED](#) | [CROSSREF](#)
18. Biswas K, Wagner Mackenzie B, Waldvogel-Thurlow S, Middleditch M, Jullig M, Zoing M, et al. Differentially regulated host proteins associated with chronic rhinosinusitis are correlated with the sinonasal microbiome. *Front Cell Infect Microbiol* 2017;7:504.
[PUBMED](#) | [CROSSREF](#)
19. Lal D, Keim P, Delisle J, Barker B, Rank MA, Chia N, et al. Mapping and comparing bacterial microbiota in the sinonasal cavity of healthy, allergic rhinitis, and chronic rhinosinusitis subjects. *Int Forum Allergy Rhinol* 2017;7:561-9.
[PUBMED](#) | [CROSSREF](#)
20. Jain R, Hoggard M, Biswas K, Zoing M, Jiang Y, Douglas R. Changes in the bacterial microbiome of patients with chronic rhinosinusitis after endoscopic sinus surgery. *Int Forum Allergy Rhinol* 2017;7:7-15.
[PUBMED](#) | [CROSSREF](#)
21. Hoggard M, Biswas K, Zoing M, Wagner Mackenzie B, Taylor MW, Douglas RG. Evidence of microbiota dysbiosis in chronic rhinosinusitis. *Int Forum Allergy Rhinol* 2017;7:230-9.
[PUBMED](#) | [CROSSREF](#)
22. Ramakrishnan VR, Gitomer S, Kofonow JM, Robertson CE, Frank DN. Investigation of sinonasal microbiome spatial organization in chronic rhinosinusitis. *Int Forum Allergy Rhinol* 2017;7:16-23.
[PUBMED](#) | [CROSSREF](#)
23. Biswas K, Hoggard M, Jain R, Taylor MW, Douglas RG. The nasal microbiota in health and disease: variation within and between subjects. *Front Microbiol* 2015;9:134.
[PUBMED](#) | [CROSSREF](#)

24. Choi EB, Hong SW, Kim DK, Jeon SG, Kim KR, Cho SH, et al. Decreased diversity of nasal microbiota and their secreted extracellular vesicles in patients with chronic rhinosinusitis based on a metagenomic analysis. *Allergy* 2014;69:517-26.
[PUBMED](#) | [CROSSREF](#)
25. Aurora R, Chatterjee D, Hentzleman J, Prasad G, Sindwani R, Sanford T. Contrasting the microbiomes from healthy volunteers and patients with chronic rhinosinusitis. *JAMA Otolaryngol Head Neck Surg* 2013;139:1328-38.
[PUBMED](#) | [CROSSREF](#)
26. Koeller K, Herlemann DPR, Schuldt T, Ovari A, Guder E, Podbielski A, et al. Microbiome and culture based analysis of chronic rhinosinusitis compared to healthy sinus mucosa. *Front Microbiol* 2018;9:643.
[PUBMED](#) | [CROSSREF](#)
27. Ramakrishnan VR, Hauser LJ, Feazel LM, Ir D, Robertson CE, Frank DN. Sinus microbiota varies among chronic rhinosinusitis phenotypes and predicts surgical outcome. *J Allergy Clin Immunol* 2015;136:334-342.e1.
[PUBMED](#) | [CROSSREF](#)
28. Fokkens WJ, Lund VJ, Mullol J, Bachert C, Alobid I, Baroody F, et al. EPOS 2012: European position paper on rhinosinusitis and nasal polyps 2012. A summary for otorhinolaryngologists. *Rhinology* 2012;50:1-12.
[PUBMED](#) | [CROSSREF](#)
29. Kim YS, Han D, Kim J, Kim DW, Kim YM, Mo JH, et al. In-depth, proteomic analysis of nasal secretions from patients with chronic rhinosinusitis and nasal polyps. *Allergy Asthma Immunol Res* 2019;11:691-708.
[PUBMED](#) | [CROSSREF](#)
30. Wiśniewski JR, Gaugaz FZ. Fast and sensitive total protein and Peptide assays for proteomic analysis. *Anal Chem* 2015;87:4110-6.
[PUBMED](#) | [CROSSREF](#)
31. Han D, Jin J, Woo J, Min H, Kim Y. Proteomic analysis of mouse astrocytes and their secretome by a combination of FASP and StageTip-based, high pH, reversed-phase fractionation. *Proteomics* 2014;14:1604-9.
[PUBMED](#) | [CROSSREF](#)
32. Woo J, Han D, Park J, Kim SJ, Kim Y. In-depth characterization of the secretome of mouse CNS cell lines by LC-MS/MS without prefractionation. *Proteomics* 2015;15:3617-22.
[PUBMED](#) | [CROSSREF](#)
33. Lee H, Kim K, Woo J, Park J, Kim H, Lee KE, et al. Quantitative proteomic analysis identifies AHNAK (neuroblast differentiation-associated protein AHNAK) as a novel candidate biomarker for bladder urothelial carcinoma diagnosis by liquid-based cytology. *Mol Cell Proteomics* 2018;17:1788-802.
[PUBMED](#) | [CROSSREF](#)
34. Bruderer R, Bernhardt OM, Gandhi T, Miladinović SM, Cheng LY, Messner S, et al. Extending the limits of quantitative proteome profiling with data-independent acquisition and application to acetaminophen-treated three-dimensional liver microtissues. *Mol Cell Proteomics* 2015;14:1400-10.
[PUBMED](#) | [CROSSREF](#)
35. Reiter L, Rinner O, Picotti P, Hüttenhain R, Beck M, Brusniak MY, et al. mProphet: automated data processing and statistical validation for large-scale SRM experiments. *Nat Methods* 2011;8:430-5.
[PUBMED](#) | [CROSSREF](#)
36. Segata N, Izard J, Waldron L, Gevers D, Miropolsky L, Garrett WS, et al. Metagenomic biomarker discovery and explanation. *Genome Biol* 2011;12:R60.
[PUBMED](#) | [CROSSREF](#)
37. Xu Z, Xu G, Pan W; Alzheimer's Disease Neuroimaging Initiative. Adaptive testing for association between two random vectors in moderate to high dimensions. *Genet Epidemiol* 2017;41:599-609.
[PUBMED](#) | [CROSSREF](#)
38. Palleja A, Mikkelsen KH, Forslund SK, Kashani A, Allin KH, Nielsen T, et al. Recovery of gut microbiota of healthy adults following antibiotic exposure. *Nat Microbiol* 2018;3:1255-65.
[PUBMED](#) | [CROSSREF](#)
39. Soyka MB, Wawrzyniak P, Eiwegger T, Holzmann D, Treis A, Wanke K, et al. Defective epithelial barrier in chronic rhinosinusitis: the regulation of tight junctions by IFN- γ and IL-4. *J Allergy Clin Immunol* 2012;130:1087-1096.e10.
[PUBMED](#) | [CROSSREF](#)
40. Khalmuratova R, Park JW, Shin HW. Immune cell responses and mucosal barrier disruptions in chronic rhinosinusitis. *Immune Netw* 2017;17:60-7.
[PUBMED](#) | [CROSSREF](#)

41. Valera FCP, Ruffin M, Adam D, Maillé É, Ibrahim B, Berube J, et al. Staphylococcus aureus impairs sinonasal epithelial repair: Effects in patients with chronic rhinosinusitis with nasal polyps and control subjects. *J Allergy Clin Immunol* 2019;143:591-603.e3.
[PUBMED](#) | [CROSSREF](#)
42. Shaw LP, Bassam H, Barnes CP, Walker AS, Klein N, Balloux F. Modelling microbiome recovery after antibiotics using a stability landscape framework. *ISME J* 2019;13:1845-56.
[PUBMED](#) | [CROSSREF](#)
43. Feng Y, Huang Y, Wang Y, Wang P, Song H, Wang F. Antibiotics induced intestinal tight junction barrier dysfunction is associated with microbiota dysbiosis, activated NLRP3 inflammasome and autophagy. *PLoS One* 2019;14:e0218384.
[PUBMED](#) | [CROSSREF](#)
44. Kohanski MA, Tharakan A, London NR, Lane AP, Ramanathan M Jr. Bactericidal antibiotics promote oxidative damage and programmed cell death in sinonasal epithelial cells. *Int Forum Allergy Rhinol* 2017;7:359-64.
[PUBMED](#) | [CROSSREF](#)
45. Yoo EJ, Ojiaku CA, Sunder K, Panettieri RA Jr. Phosphoinositide 3-kinase in asthma: novel roles and therapeutic approaches. *Am J Respir Cell Mol Biol* 2017;56:700-7.
[PUBMED](#) | [CROSSREF](#)
46. Gaudette BT, Jones DD, Bortnick A, Argon Y, Allman D. mTORC1 coordinates an immediate unfolded protein response-related transcriptome in activated B cells preceding antibody secretion. *Nat Commun* 2020;11:723.
[PUBMED](#) | [CROSSREF](#)
47. Finney LJ, Belchamber KBR, Fenwick PS, Kemp SV, Edwards MR, Mallia P, et al. Human rhinovirus impairs the innate immune response to bacteria in alveolar macrophages in chronic obstructive pulmonary disease. *Am J Respir Crit Care Med* 2019;199:1496-507.
[PUBMED](#) | [CROSSREF](#)
48. Tan HY, Wang N, Li S, Hong M, Wang X, Feng Y. The reactive oxygen species in macrophage polarization: reflecting its dual role in progression and treatment of human diseases. *Oxid Med Cell Longev* 2016;2016:2795090.
[PUBMED](#) | [CROSSREF](#)
49. Higham A, Lea S, Plumb J, Maschera B, Simpson K, Ray D, et al. The role of the liver X receptor in chronic obstructive pulmonary disease. *Respir Res* 2013;14:106.
[PUBMED](#) | [CROSSREF](#)
50. Matalonga J, Glaria E, Bresque M, Escande C, Carbó JM, Kiefer K, et al. The nuclear receptor LXR limits bacterial infection of host macrophages through a mechanism that impacts cellular NAD metabolism. *Cell Reports* 2017;18:1241-55.
[PUBMED](#) | [CROSSREF](#)